ISSN 1027-4510, Journal of Surface Investigation: X-ray, Synchrotron and Neutron Techniques, 2020, Vol. 14, Suppl. 1, pp. S69–S74. © Pleiades Publishing, Ltd., 2020.

How Neutrons Facilitate Research into Gas Turbines and Batteries from Development to Engineering Applications

R. Gilles[a,*]

[a]*Heinz Maier-Leibnitz Zentrum, Technische Universität München, Garching, 85748 Germany*

**e-mail: ralph.gilles@frm2.tum.de*

Received July 23, 2019; revised August 18, 2019; accepted August 21, 2019

Abstract—This contribution presents an overview of how neutrons support the development of gas turbine materials and batteries due to their unique properties of being non-destructive, having a large beam cross section, offering relatively high sensitivity to light elements in the neighborhood of heavy elements and proving suitable for in situ and/or operando studies. Various neutron techniques, together with sophisticated sample environments, are applied to measure materials under real working conditions. For gas turbines, the focus is on the in situ characterization of the strengthening precipitates of high-temperature alloys at elevated temperatures. Battery research using neutrons deals mainly with the observation of Li movements and distributions, e.g., during charging and discharging of a cell or under the influence of an external parameter, such as temperature.

Keywords: neutron diffraction, small-angle neutron scattering, neutron imaging, superalloy, gas turbine, battery

DOI: 10.1134/S1027451020070162

INTRODUCTION

The relentless growth in population and industry has led to an unprecedented global increase in the demand for energy and mobility. Meeting these requirements necessitates supplying far more energy and transportation, and doing so more efficiently. Despite an abundance of possibilities for generating new types of power – especially in the field of renewable energies – the burning of fossil fuels will play a central role in emerging economies in the coming decades. Consequently, it is crucial that power-generating heat engines are as efficient as possible. Gas turbines for aircraft and stationary power engines, as well as batteries for electromobility and consumer electronics, are two key technological fields for research.

RESULTS AND DISCUSSION

Gas Turbines

In the field of high-temperature alloy applications, gas turbines play a significant role in terms of energy conversion. In particular, improvements to Ni-based and Co-based superalloys from wrought to cast alloys that have excellent properties in regard to high-temperature strength or corrosion and creep resistance, including high fracture toughness, are a case in point. The main goal of existing superalloys is to increase the operating temperature of these alloys in gas turbines [1] to allow engine manufacturers to improve fuel efficiency. Most superalloys consist of so-called γ' precipitates in a γ matrix plus additional high-temperature phases [2]. The last few decades have seen the scientific community put great effort into the development of superalloys for stationary gas turbines with operating temperatures above 650°C whilst keeping the good processing characteristics of the well-known superalloy 718. In addition, new alloy concepts, such as the CoRe alloys with TaC precipitates [3], have been investigated with a view to enhancing the service temperature and optimizing the precipitation stability and size [4]. Neutron methods [5–7] support these improvements through various techniques (Fig. 1). In situ neutron diffraction is a tool to identify all contributing phases [5]. Neutron diffraction is an interaction of neutrons with the nucleus of an atom. Neutrons possess quite different sensitivity to chemical elements in comparison with other probes, as for example electrons [8] or X-rays [9]. This is important if the superlattice structures of precipitates are under investigation because these phases can have very weak reflections from the ordering of atoms and their low volume fraction [2]. In general, nano-scaled precipitates in Ni-based alloys have an ordered $L1_2$ structure of $NiAl_3$ type, which are coherently embedded in an unordered face-centered cubic Ni-matrix. This means that many diffraction peaks overlap and a few additional peaks result from the superlattice structure of the precipitates due to the ordering. Complementary neutron and X-ray diffraction patterns are often necessary to determine the lattice parameters and the misfit (lattice mismatch of the two phases of precipitates and matrix)

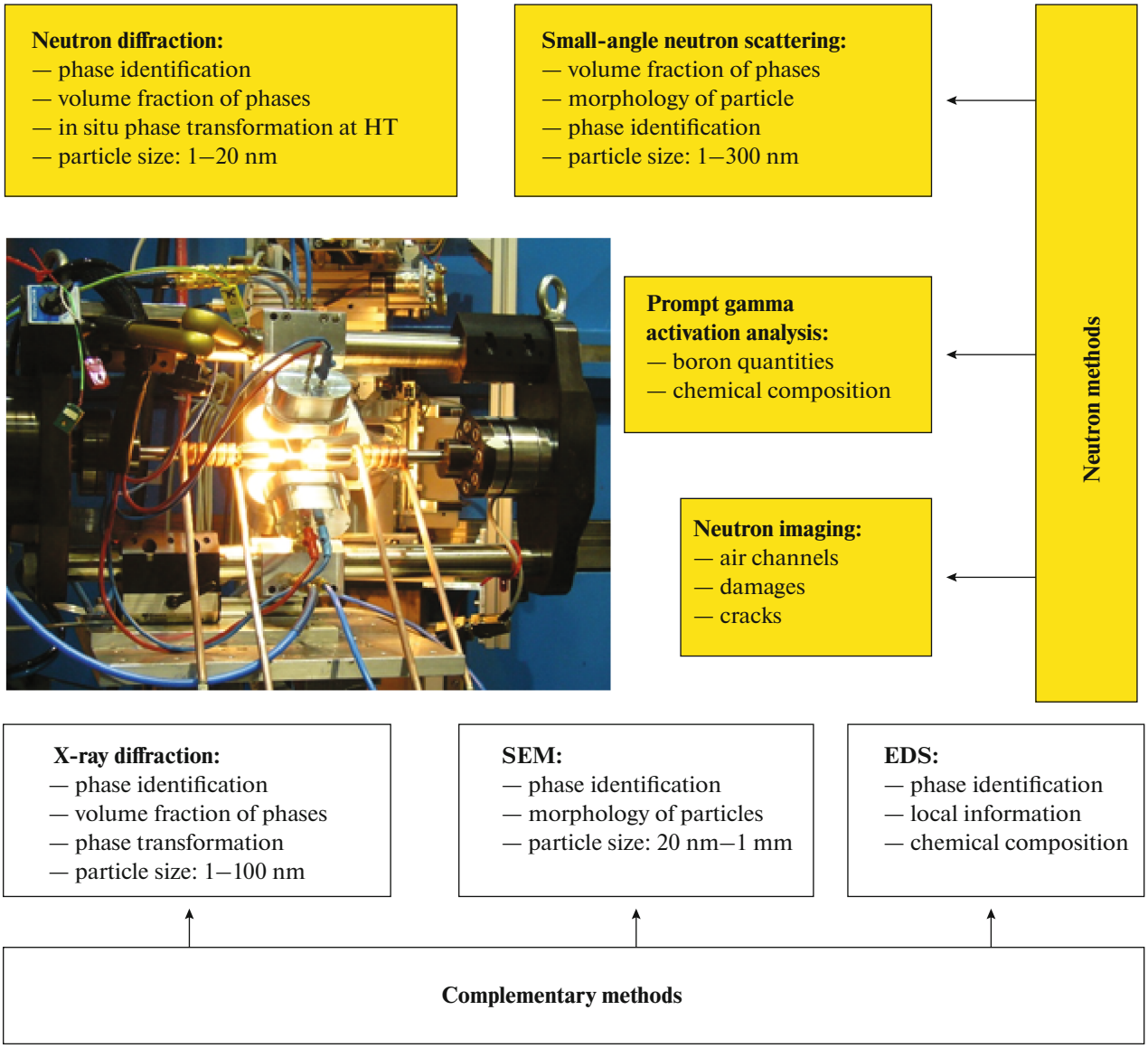

Fig. 1. A tensile rig with a high-temperature furnace installed at the Stress-Spec instrument @ Heinz Maier–Leibnitz Zentrum. High-temperature alloys are measured simultaneously under heat treatment and tension or pressure. Top and right: typical neutron methods and their application for high-temperature alloy studies; bottom: complementary methods of X-ray diffraction and microscopy including their application in the field of high-temperature alloys.

[10, 11] which is directly correlated to the stability of the alloy and morphology of the precipitates. Due to the application of high-temperature alloys, experiments are often carried out under high temperatures to characterize all crystallographic phases (including carbides and phase transformations which typically occur at very high temperatures) involved in the alloy under service condition [12]. All phases influence each other and determine the overall performance of the alloy, defining the high mechanical strength, the surface stability at high temperatures and the oxidation and creep resistance. In particular, the evolution of precipitates under holding at certain high temperatures or under a change of temperatures is the focus of the current research [4]. In addition, to simulate the condition of a gas turbine in operation, loading experiments are performed to determine the strength or strain of the alloy under loading [13] or compression [14]. Neutron diffraction is limited to 1–20 nm for the characterization of precipitate size owing to the instrument resolution being strongly correlated to the monochromator wavelength distribution.

With small-angle neutron scattering (SANS) [15, 16], a technique is used which provides sensitivity on a larger range of the nanometer scale (1–300 nm). Neutrons are scattered around the primary beam at small angles. The SANS method collects the measured intensity resulting from the scattering contrast of

embedded nano-scaled objects in a matrix [7]. Precipitates in respect of the size and the volume fraction including their distributions and the morphologies (spheres, cubes, plates or needles are typical shapes for high-temperature precipitates) can be described in more detail under the influence, e.g., of small composition changes or different heat treatments [17, 18]. SANS at high temperatures makes it possible to follow the dissolution of precipitates and during cooling to describe the forming of precipitate dependence on the cooling rate or temperature sequence, including holding at certain temperatures [19].

Using the neutron imaging technique [20, 21] involves placing a detector after the sample and illuminating an object to measure the neutron attenuation caused by the sample material. The image obtained is a 2D radiography of the object. If the object is rotated to various positions, a summation of radiography images can be performed for a 3D tomography image. Sophisticated software allows conducting intersections of the object to achieve better information on the interior. Applications such as cracks or air channels are studied from around <100 μm or mm, respectively, up to many centimeters in gas turbine blades [22]. Here, the advantage of using neutrons is that, especially in the case of metals, the relatively weak attenuation of the neutron beam offers the possibility of radiography and tomography experiments on objects with relatively large thicknesses. For very large objects, fast neutrons with higher energies having deeper penetration depths are applied to achieve higher transmissions of the neutrons.

The use of neutron-induced prompt gamma activation analysis [23] is an indirect use of neutrons. A neutron is captured from a nucleus and leads to a nuclear excitation at a higher energy level. The relaxation to the ground level via the emission of a specific γ radiation makes it possible to identify the chemical element reacting with the neutron through the specific γ line. As the method is quite sensitive to a few very light elements, it is suited, for example, to the determination of boron quantities in superalloys [24], which is important for understanding the strengthening at grain boundaries.

Nevertheless, complementary methods, such as microscopy (SEM, TEM and EDS) or X-ray diffraction, together with neutron methods, are often necessary to understand a complex microstructure well [2, 4, 12, 18] over different length scales and to glean information not only from reciprocal space, but from direct space, too.

Batteries

In order to gain a better understanding of the electrochemistry in batteries, a huge demand has emerged for in situ and operando characterization methods. Due to the high penetration depth and high sensitivity of neutrons to light elements such as lithium, a probe of this nature has become ever more attractive over the last decade [25]. The present contribution gives an overview as to how neutrons, with their unique properties, contribute to the development of new battery cell types (Fig. 2). During the charging and discharging of cells, the intercalation of Li in the graphite layers can be observed with in situ neutron diffraction, as such measurements are able to detect LiC_x phases, such as LiC_6 and LiC_{12}, during the intercalation/deintercalation process [26]. Such experiments allow the estimations of the amount of Li in the anode. This is of great importance as the formation process and cycling consume Li, for example, to build up a passive protective layer (Solid Electrolyte Interface, or SEI) between the electrode and electrolyte [27]. Similar considerations are possible when studying the chemical structure of the cathode, for example the NiMnCo electrode [28]. Implemented Li changes the structure slightly and here neutrons can easily distinguish between the three neighboring elements of the periodic table due to different sensitivity. Under fast charging conditions and low temperatures, the appearance of Li plating can occur and influences the cell performance in a negative way. Li plating is an accumulation of highly reactive metallic Li on the surface of the electrode. Fast charging and low temperatures result in a jam for the Li diffusion in the electrode. After a relaxation time, very often more or less full lithiation takes place, removing all metallic lithium [29, 30]. If, however, dendrides of Li are formed, this can lead to a short circuit resulting in the worst case to a burn-up. Electric cars, mobile phones and nowadays e-cigarettes have already shown this phenomenon.

On larger scales of the order of >50 μm, neutron imaging (radiography and tomography) facilitates a non-destructive view inside the cell, even for batteries having a steel casing. As an example of such a battery type, ZEBRA (Zero Emission Battery Research Activities) cells [31, 32] were measured, as they are an attractive alternative to conventional batteries because of the high safety of the sodium metal halide and low costs. Mobile applications, such as hybrid locomotives, benefit from these batteries. The cathode consists of a mixture of NaCl, metal (Fe and/or Ni) and $NaAlCl_4$ filled into an alumina tube. At cell operation temperature between 270–350°C, the salt $NaAlCl_4$ is molten and serves as an electrolyte while nickel wire (positive electrode) is used as the current collector. The cell reaction is: $2NaCl + Metal \rightarrow Metal\ Cl_2 + 2Na$. The liquid Na is the negative electrode. The filling level of the sodium in the battery can be observed via a sequence of radiography images during charging and discharging and directly correlated to the charging status of the cell [33]. A similar application is to follow the distribution of the electrolyte during the filling process of the cell under the condition of a layer

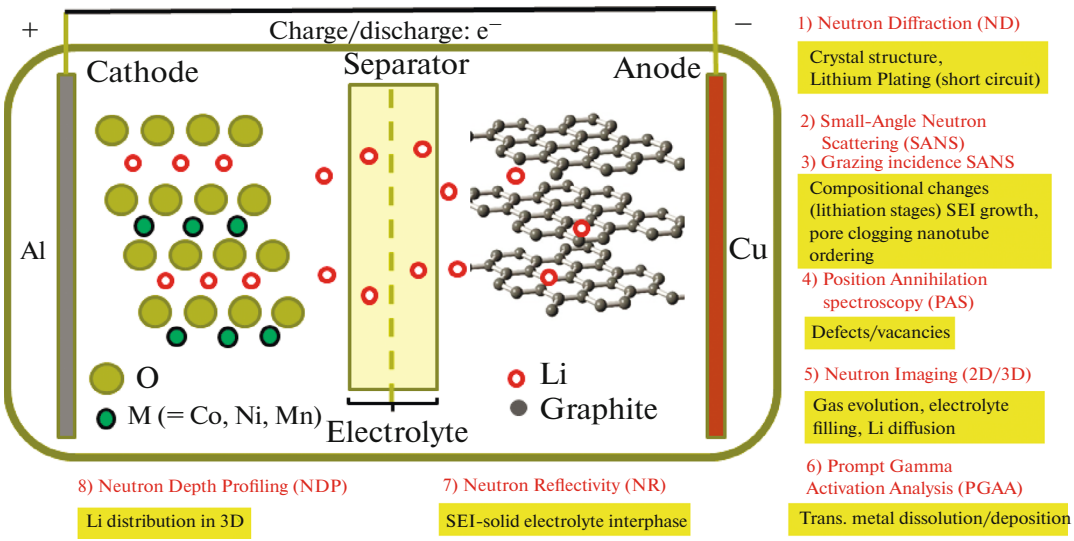

Fig. 2. Schematic drawing of a Li-ion cell with graphite and metal oxide electrode. Right and bottom: various neutron methods or derived methods using neutrons to create other probes (prompt gamma activation analysis and positron annihilation spectroscopy) and their typical applications for Li-ion batteries.

stacked pouch cell [34]. There is a real industrial motivation behind this. In industrial processes, it is very important to fill cells as fast as possible and in a homogenous way, so that air is not trapped and the pressure is not too high. Typical questions which will be answered are how the soaking of the electrolyte in the cell works, how the wetting process on the layer stack takes place, which pathways of the liquid in the cell are used depending on the cell geometry. Optimization of dosing, pressure, and venting are carried out for each cell type to save time in the battery production line. The time needed for the filling process of hard case prismatic cells can be reduced by up to 50% after optimization with neutrons [35].

The method of prompt gamma activation analysis with sufficiently high sensitivity to detect small amount of elements is a powerful tool to describe the capacity loss of the cells if a tiny amount of metal (in the order of ppm level) is deposited on the graphite anode after the charging/discharging processes. Here, the different sensitivity to Ni, Mn and Co for neutron capture allows quantifying the relative amount of each element even on the ppm level. In addition, the influence of temperature and voltage on the deposition amount of the three metals was studied during the cycling process [36].

Neutron depth profiling [37] is a rediscovered method, which is very kind to the surfaces. Neutrons and Li atoms react to two charged particles, a triton and a α particle both sent out in opposite directions [38] and detected via germanium detectors. Irradiated materials with neutron beams allow only certain nuclides to emit charged particles after neutron capture (^{3}He, ^{6}Li, ^{10}B, ^{14}N, ^{17}O, ^{33}S, ^{35}Cl, and ^{40}K, as well as a few radioactive nuclides: ^{7}Be, ^{22}Na and ^{59}Ni) [39]. Due to the easy energy loss of the two charged particles in materials, the depth position of the reaction can be determined. For high resolution (a few nanometers), α particles are used for studies of the first about 10 μm, while for a thickness up to approximately 100 μm (depending on the material), triton particles of less resolution are used [40]. Extracted graphite electrodes of different cycled cells were studied with respect to the SEI layer thickness and the Li gradient in the layer itself [41, 42].

Operando SANS experiments on thin Li-ion pouch cells have been performed to understand in more detail the SEI formation [43], the lithiation process of Li in graphite [44] and the pore clogging of the electrolyte and SEI in porous Si-graphite electrodes [45]. The deuteration of cell components in SANS experiments significantly expand the results. A modified method of SANS, called grazing incidence small-angle neutron scattering [46], is very helpful to gain information on nanotube arrays as self-organized anodic titania (TiO_2) tubes for anode materials. Nanotube separation distances and diameter of tubes can be measured with good precision because a beam spot up to a few cm^2 can be applied [47].

Neutron reflectivity [48, 49] is adopted for surface studies to detect interlayers and Li distributions on thin smooth film batteries using a parallel neutron beam reflected on a layer stack of a cell. Typical examples of measurements on operando cells are the observation of the electrochemical incorporation of Li into a crystalline [50] or amorphous Si anode [51] and the growth of the SEI layer [52] under charging and discharging conditions.

Another indirect method using neutrons is that of positron annihilation spectroscopy [53]. Neutrons

converted to positrons stand out with very high sensitivity to surface defects such as vacancies. Irreversible capacity loss of the cathode material can be related to lithium vacancies (measured via positrons) as a kinetic hindrance in the relithiation behavior, for example, of Li in NiMnCo electrodes [54].

CONCLUSIONS

Neutrons as a probe are a very suitable tool to study gas turbines (high-temperature alloys) and battery cells, including their individual components. The manifold properties of neutrons, including deep penetration depth, good sensitivity to light elements and the possibility of applications over a large length scale (sub-nanometer to centimeter) using different techniques, enable measurements starting from single components up to complete energy systems. This includes receiving information on the interior without destroying the measured object. In particular, in situ and operando experiments strongly support the conventional methods (e.g., microscopy) for the understanding and further development of a single component, as well as of the whole system such as a complete gas turbine or a battery cell.

REFERENCES

1. J. H. Perepezko, Science **326**, 1069 (2009).
2. R. Gilles, Int. J. Mater. Res. **96**, 325 (2005).
3. J. Rösler, D. Mukherji, and D. Baranski, Adv. Eng. Mater. **9**, 876 (2007).
4. R. Gilles, D. Mukherji, L. Karge, P. Strunz, P. Beran, B. Barbier, A. Kriele, M. Hofmann, H. Eckerlebe, and J. Rösler, J. Appl. Crystallogr. **49**, 1253 (2016).
5. G. E. Bacon, *Neutron Diffraction* (Clarendon, Oxford, 1975).
6. G. L. Squires, *Introduction to the Theory of Thermal Neutron Scattering* (Cambridge University Press, Cambridge, 1978).
7. G. Kostorz, Treatise Mater. Sci. Technol. **15**, 227 (1979).
8. B. K. Vainshtein, *Structure Analysis by Electron Diffraction* (Pergamon, Oxford, 1964).
9. B. E. Warren, *X-Ray Diffraction* (Dover, New York, 1990).
10. A. G. Khachaturyan, S. V. Semenovskaya, and J. W. Morris, Acta Metall. **36**, 1563 (1998).
11. R. Gilles, D. Mukherji, P. Strunz, B. Barbier, D. M. Többens, and J. Rösler, Appl. Phys. A: Mater. Sci. Process. **74**, 1446 (2002).
12. D. Mukherji, P. Strunz, R. Gilles, M. Hofmann, F. Schmitz, and J. Rösler, Mater. Lett. **64**, 2608 (2010).
13. J. von Kobylinski, R. Lawintzki, M. Hofmann, C. Krempaszky, and E. Werner, Continuum Mech.Thermodyn. **31** (3), 691 (2019).
14. Z. Zhang, Y. Feng, Q. Tan, J. Zou, J. Li, X. Zhou, G. Sun, and Y. Wang, Mater. Des. **166**, 107603 (2019).
15. A. Guinier and G. Fournet, *Small-Angle Scattering of X-Rays* (Wiley, New York, 1955).
16. L. A. Feigin and D. I. Svergun, *Structure Analysis by Small-Angle X-ray and Neutron Scattering* (Plenum, New York, 1987).
17. L. Karge, R. Gilles, D. Mukherji, P. Strunz, M. Hofmann, J. Gavilano, U. Keiderling, O. Dolotko, A. Kriele, A. Neubert, J. Rösler, and W. Petry, Acta Mater. **132**, 354 (2017).
18. L. Karge, D. Lang, J. Schatte, R. Gilles, S. Busch, P. Leibenguth, H. Clemens, and W. Petry, J. Appl. Crystallogr. **51**, 1706 (2018).
19. R. Gilles, D. Mukherji, H. Eckerlebe, L. Karge, P. Staron, P. Strunz, and Th. Lippmann, J. Alloys Compd. **612**, 90 (2014).
20. I. S. Anderson, R. M. Greevy, and H. Z. Bilheux, *Neutron Imaging and Applications: A Reference for the Imaging Community* (Springer, New York, 2009).
21. N. Kardjilov, I. Manke, A. Hilger, M. Strobl, and J. Banhart, Mater. Today **14**, 248 (2011).
22. S. Peetermans and E. H. Lehmann, NDT&E Int. **79**, 109 (2016).
23. Z. Revay and T. Belgya, *Handbook of Prompt Gamma Activation Analysis* (Springer, Boston, 2004), p. 1.
24. D. Mukherji, J. Rösler, M. Krüger, M. Heilmaier, M. C. Bölitz, R. Völkl, U. Glatzel, and L. Szentmiklosi, Scr. Mater. **66**, 60 (2012).
25. D. Liu, Z. Shadike, R. Lin, K. Qian, H. Li, K. Li, S. Wang, Q. Yu, M. Liu, S. Ganapathy, X. Qin, Q. H. Yang, M. Wagemaker, F. Kang, X. Q. Yang, and B. Li, Adv. Mater. **31**, 1806620 (2019).
26. V. Zinth, C. von Lüders, M. Hofmann, J. Hattendorff, I. Buchberger, S. V. Erhard, J. R. Kornmeier, A. Jossen, and R. Gilles, J. Power Sources **271**, 152 (2014).
27. N. Paul, J. Wandt, S. Seidlmayer, S. Schebesta, M. J. Mühlbauer, O. Dolotko, H. A. Gasteiger, and R. Gilles, J. Power Sources **345**, 85 (2017).
28. N. Paul, J. Keil, F. M. Kindermann, S. Schebesta, O. Dolotko, M. J. Mühlbauer, L. Kraft, S. V. Erhard, A. Jossen, and R. Gilles, J. Energy Storage **17**, 383 (2018).
29. C. von Lüders, V. Zinth, S. V. Erhard, P. J. Osswald, M. Hofmann, R. Gilles, and A. Jossen, J. Power Sources **342**, 17 (2017).
30. V. Zinth, C. von Lüders, J. Wilhelm, S. V. Erhard, M. Hofmann, S. Seidlmayer, J. Rebelo-Kornmeier, W. Gan, A. Jossen, and R. Gilles, J. Power Sources **361**, 54 (2017).
31. J. Coetzer, J. Power Sources **18**, 377 (1986).
32. J. L. Sudworth, J. Power Sources **100**, 149 (2001).
33. V. Zinth, M. Schulz, S. Seidlmayer, N. Zanon, R. Gilles, and M. Hofmann, J. Electrochem. Soc. **163**, A838 (2016).
34. T. Knoche, V. Zinth, M. Schulz, J. Schnell, R. Gilles, and G. Reinhart, J. Power Sources **331**, 267 (2016).
35. W. Weydanz, H. Reisenweber, A. Gottschalk, M. Schulz, T. Knoche, G. Reinhart, M. Masuch, J. Franke, and R. Gilles, J. Power Sources **380**, 126 (2018).

36. I. Buchberger, S. Seidlmayer, A. Pokharel, M. Piana, J. Hattendorff, P. Kudejova, R. Gilles, and H. A. Gasteiger, J. Electrochem. Soc. **162**, A2737 (2015).
37. J. F. Ziegler, B. L. Crowder, G. E. Cole, J. E. E. Baglin, and B. J. Masters, Appl. Phys. Lett. **21**, 16 (1972).
38. G. Downing and G. P. Lamaze, Semicond. Sci. Technol. **10**, 1423 (1995).
39. G. Downing, G.P. Lamaze, J. Langland, and S. Hwang, J. Res. Natl. Inst. Stand. Technol. **98**, 109 (1993).
40. L. Werner, M. Trunk, L. Werner, R. Gilles, B. Märkisch, and Z. Revay, Nucl. Instrum. Methods Phys. Res., Sect. A **911**, 30 (2018).
41. M. Wetjen, M. Trunk, L. Werner, R. Gernhäuser, B. Märkisch, Z. Revay, R. Gilles, and H. A. Gasteiger, J. Electrochem. Soc. **165**, A2340 (2018).
42. M. Trunk, M. Wetjen, L. Werner, R. Gernhäuser, B. Märkisch, Z. Revay, H. A. Gasteiger, and R. Gilles, Mater. Charact. **146**, 127 (2018).
43. C. A. Bridges, X. G. Sun, J. Zhao, M. P. Paranthaman, and S. Dai, J. Phys. Chem. C **116**, 7701 (2012).
44. S. Seidlmayer, J. Hattendorff, I. Buchberger, L. Karge, H. A. Gasteiger, and R. Gilles, J. Electrochem. Soc. **162**, A3116 (2015).
45. N. Paul, J. Brumbarov, A. Paul, Y. Chen, J. F. Moulin, P. Müller-Buschbaum, J. Kunze-Liebhäuser, and R. Gilles, J. Appl. Crystallogr. **48**, 444 (2015).
46. P. Müller-Buschbaum, Polym. J. **45**, 34 (2013).
47. N. Paul, M. Wetjen, S. Busch, H. A. Gasteiger, and R. Gilles, J. Electrochem Soc. **166**, A1051 (2019).
48. I. W. Hamsley and J. S. Pedersen, J. Appl. Crystallogr. **27**, 29 (1994).
49. J. S. Pedersen and I. W. Hamsley, J. Appl. Crystallogr. **27**, 36 (1994).
50. B. K. Seidlhofer, B. Jerliu, M. Trapp, E. Hüger, S. Risse, R. Cubitt, H. Schmidt, R. Steitz, and M. Ballauff, ACS Nano **10**, 7458 (2016).
51. B. Jerliu, L. Dörrer, E. Hüger, G. Borchardt, R. Steitz, U. Geckle, V. Oberst, M. Bruns, O. Schneider, and H. Schmidt, Phys. Chem. Chem. Phys. **15**, 7777 (2013).
52. H. Kawaura, M. Harada, Y. Kondo, H. Kondo, Y. Suganuma, N. Takahashi, J. Sugiyama, Y. Seno, and N. Yamada, ACS Appl. Mater. Interfaces **8**, 9540 (2016).
53. R. W. Siegel, Annu. Rev. Mater. Sci. **10**, 393 (1980).
54. S. Seidlmayer, I. Buchberger, M. Reiner, T. Gigl, R. Gilles, H. A. Gasteiger, and C. Hugenschmidt, J. Power Sources **336**, 224 (2016).